J. Anat. (2008) **212**, pp286–294 doi: 10.1111/j.1469-7580.2008.00853.x

Chronic right ventricular pressure overload results in a hyperplastic rather than a hypertrophic myocardial response

Boudewijn P. J. Leeuwenburgh,[1,2] Willem A. Helbing,[2] Arnold C. G. Wenink,[3] Paul Steendijk,[1] Roos de Jong,[1] Enno J. Dreef,[4] Adriana C. Gittenberger-de Groot,[3] Jan Baan[1] and Arnoud van der Laarse[1]

[1]*Departments of Cardiology,* [2]*Pediatric Cardiology,* [3]*Anatomy and Embryology and* [4]*Pathology of the Leiden University Medical Center, Leiden, The Netherlands*

Abstract

Myocardial hyperplasia is generally considered to occur only during fetal development. However, recent evidence suggests that this type of response may also be triggered by cardiac overload after birth. In congenital heart disease, loading conditions are frequently abnormal, thereby affecting ventricular function. We hypothesized that chronic right ventricular pressure overload imposed on neonatal hearts initiates a hyperplastic response in the right ventricular myocardium. To test this, young lambs (aged 2–3 weeks) underwent adjustable pulmonary artery banding to obtain peak right ventricular pressures equal to left ventricular pressures for 8 weeks. Transmural cardiac tissue samples from the right and left ventricles of five banded and five age-matched control animals were studied. We found that chronic right ventricular pressure overload resulted in a twofold increase in right-to-left ventricle wall thickness ratio. Morphometric right ventricular myocardial tissue analysis revealed no changes in tissue composition between the two groups; nor were right ventricular myocyte dimensions, relative number of binucleated myocytes, or myocardial DNA concentration significantly different from control values. In chronic pressure overloaded right ventricular myocardium, significantly ($P < 0.01$) more myocyte nuclei were positive for the proliferation marker proliferating cellular nuclear antigen than in control right ventricular myocardium. Chronic right ventricular pressure overload applied in neonatal sheep hearts results in a significant increase in right ventricular free wall thickness which is primarily the result of a hyperplastic myocardial response.

Key words hypertension; hypertrophy; morphometry; myocardial hyperplasia; right ventricle.

Introduction

It is generally believed that the adult cardiac myocyte is a terminally differentiated cell which has lost its ability of mitotic division (e.g. hyperplastic growth) (Becker, 1993). Myocardial hypertrophy is considered to be the mechanism by which the (adult) heart compensates for an increase in workload, that is, by increasing the size of existing myocytes. In contrast, in fetal hearts hyperplastic growth is the prevalent means of myocardial growth by which new myocytes are added to the myocardium (Saiki et al. 1997). Shortly after birth, when loading conditions of the heart change, a shift from predominantly hyperplastic growth to hypertrophic growth occurs (Clubb et al. 1984; Rakusan, 1984; Beinlich et al. 1995; Li et al. 1996). The exact timing of this transition is subject to debate. In patients with congenital heart disease, however, abnormal cardiac anatomy may result in a situation in which ventricular loading conditions may be increased for a prolonged period of time. Accordingly, it may be hypothesized that in these hearts a hyperplastic growth pattern may (co)exist for a prolonged period of time. This hypothesis may be supported by several studies that have questioned the dogma that after birth, hypertrophic growth is the predominant myocardial response to increased loading conditions (Astorri et al. 1971; Bishop & Hine, 1975; Oparil et al. 1984; Olivetti et al. 1987, 1988, 1994; Anversa et al. 1992; Grajek et al. 1993; Sedmera et al. 2003). In 2-month-old-rats, Olivetti et al. (1988) showed that pulmonary artery banding (PAB) resulted in increased cellular diameter but also in an increased number of myocytes, indicative of myocyte hyperplasia. Grajek et al. (1993) studied 103 human hearts with various forms of muscle hypertrophy and, based on morphometric measurements, found marked signs of myocyte hyperplasia in all hearts weighing more than 350 g, irrespective of the aetiology of hypertrophy.

Extended hyperplastic growth is a vital component of ventricular wall restructuring, and, as such, may have important influences on overall cardiac pump function in pathological circumstances such as pressure overload (Anversa & Kajstura, 1998; Gerdes, 2002). Although a reasonable body of research has been performed on the effects of pressure overload in

Correspondence
A. van der Laarse, PhD, Department of Cardiology, C5-P, Leiden University Medical Center, P.O. Box 9600, 2300 RC Leiden, The Netherlands. T: +31 715262020; F: +31 715266809; E: a.van_der_laarse@lumc.nl

Accepted for publication *6 December 2007*

the adult heart, little is known about these effects in the young heart subject to ventricular overload, particularly in the presence of congenital heart disease.

The aim of this study was to investigate the cellular and biochemical myocardial responses to chronic right ventricular (RV) pressure overload that was given to young lambs by means of adjustable pulmonary artery banding for a period of 8 weeks. The hemodynamic effects of this pressure overload have been described elsewhere (Leeuwenburgh et al. 2001, 2002). We hypothesized that chronic RV pressure overload, applied at a young age in lambs, resulted primarily in a RV myocardial hyperplastic response rather than in a hypertrophic response. The effects of chronic RV pressure overload were characterized by means of morphometric techniques of transmural RV and left ventricular (LV) myocardial tissue samples and individual RV myocytes, as well as biochemical analysis of myocardial tissue of LV and RV free wall and interventricular septum (IVS) samples. Immunohistochemical staining for a proliferation marker, proliferating cellular nuclear antigen (PCNA), was applied to detect a myocardial hyperplastic response in RV myocardium.

Methods

Cardiac tissue was obtained from hearts of lambs enrolled in a hemodynamic study of chronic RV pressure overload which has been outlined in detail elsewhere (Leeuwenburgh et al. 2001). Animal treatment followed the guidelines in the *Guide for the Care and Use of Laboratory Animals* (National Institute of Health Publication No. 85–23, revised 1996). The research protocol was approved by the animal research committee of the Leiden University Medical Center.

In brief, five young lambs (age 2–3 weeks, mean body mass 6.4 ± 1.7 kg) were subjected to progressive pulmonary artery banding using an inflatable cuff. RV pressure was increased to systemic (aortic) level by gradual inflation of the cuff over a 2-week period. As soon as peak systolic RV pressure averaged peak systolic aortic pressure, this pressure overload was maintained for an 8-week period (Leeuwenburgh et al. 2001). Five age-matched lambs served as controls.

Tissue collection

After 8 weeks of chronic RV pressure overload (mean 64 ± 8 days), transmural tissue blocks of the RV free wall, LV free wall and IVS were excised from the hearts of five RV pressure overloaded lambs and five age-matched control lambs. Each tissue block was cut in two transmural parts, one of which was immediately snap-frozen in liquid nitrogen and stored at –80 °C for analysis later on. The other part was fixed in ethanol–acetic acid (2% v/v) for 24 h and embedded in paraffin. Sections were cut at 5 μm in the transmural plane and stained with Haematoxylin and Eosin (HE) and a modified Von Gieson staining solution to visualize collagen.

Histomorphometry

Relative volume fractions of cardiac myocytes, cardiac myocyte nuclei, collagen, tissue gaps and other structures (including endothelial cells) were determined using the principle that the volume fraction of a certain tissue component equals the number of points of a point grid coinciding with this structure, divided by the total number of grid points (Weibel, 1979).

In each section, a distinction was made between epicardial, mid-myocardial and endocardial layers. In each of these three layers, 12 different fields were measured which were divided over three consecutive sections (50 μm apart). Thus, for each tissue sample, a total of 36 fields were counted. Within each field, several grids with variable density of points were used to count the structures mentioned before. The grids (10 × 10 cm in size) were scaled down in size by a factor of 100 and projected over the field of interest using a side-viewing arm that was attached to the microscope. The density of points within each 10 × 10 cm grid was dependent on the structure to be counted and was based on having at least 100 hits per structure per layer: 4 × 4 (myocytes), 10 × 10 (collagen and tissue gaps) and 20 × 20 points (myocyte nuclei). Starting arbitrarily in the upper part of each layer of a section, the section was consecutively moved down over a fixed distance to count the other three fields per section. Vascular lumen was not counted as tissue gap.

Cardiomyocyte isolation

To determine whether one or more nuclei were present within a single cardiac myocyte, cardiac myocytes were isolated from paraffin-embedded sections (> 100 μm thick). Tissue sections were deparaffinized and rehydrated using standard histological techniques. During gentle rotation in a rotary shaker, the tissue was shaken at 37 °C with 5 mL collagenase solution (450 U mL^{-1}, Worthington, type I) and some glass beads. After 30 min, the collagenase solution was replaced by 5 mL of fresh collagenase solution for another 30 min. Myocytes were harvested by centrifugation (100 *g*, 10 min). The supernatant was removed and the cells were resuspended in phosphate-buffered saline. In a cytospin centrifuge (120 *g*, 10 min), the cells were transferred to a glass slide and stained with HE. Cell dimensions of 25 individual myocytes per slide and number of nuclei per myocyte were determined by light microscopy. Myocyte area was estimated by multiplying myocyte length by myocyte width.

Immunohistochemistry

To determine the density of proliferating myocytes, two tissue sections per RV sample were deparaffinized, followed by blocking endogenous peroxidase activity by incubation

in 0.3% hydrogen peroxide/methanol solution for 20 min. Due to the small size of one tissue sample, only one slide could be made from one of the RV overload samples. Antigen unmasking was performed by treating the sections with boiling sodium citrate buffer (0.01 M, pH 6.0) in a microwave oven at maximal power for 13 min (Norton, 1993). The sections were left at room temperature for 2 h, followed by incubation overnight with a primary mouse anti-PCNA antibody (Sigma, Zwijndrecht, The Netherlands, dilution 1 : 400 000). Next, biotin-labelled rabbit anti-mouse secondary antibody (DakoCytomation, Glostrup, Denmark, dilution 1 : 200) was added for 30 min followed by incubation with peroxidase conjugated to streptavidin (K0377, DakoCytomation) for 30 min. Sections were treated with DAB solution (Sigma) and stained with HE.

Of each section, two series of photographs (width $\times$ height $= 0.25 \times 0.19$ mm) were taken randomly. Using image analysis software (ImagePro, Media Cybernetics, Silver Spring, MD, USA), both the number of PCNA-positive myocyte nuclei as well as the total number of myocyte nuclei were counted and used to calculate the fraction of PCNA-positive myocyte nuclei. This analysis was blindly performed by an external observer.

Sample preparation for biochemical analysis

From frozen tissue blocks of the LV and RV free wall and IVS, samples of approximately 25 mg were excised and homogenized using an Ultra-Turrax® (Janke & Kunkel, Staufen im Breisgrau, Germany) in 2.5 mL of buffer solution containing 62.5 mM Tris-HCl (pH 6.8), 15 mM dithiothreitol, 0.1 mM PMSF, 0.5 mM leupeptin, 1% (w/v) SDS and 15% (v/v) glycerol, and stored at –20 °C until use.

Determination of DNA content

Per sample, 500 μL of tissue homogenate was mixed with 1.0 mL ribonuclease A (25 μg mL^{-1}, Calbiochem, Merck Chemicals Ltd, Nottingham, UK), 500 μL Pronase (100 μg mL^{-1}, Roche, Almere, The Netherlands) and 500 μL ethidium bromide (25 μg mL^{-1}, Molecular Probes, Invitrogen, Breda, The Netherlands). The DNA concentration of the tissue homogenate was measured using a spectrofluorometer (Perkin-Elmer LS-3, Groningen, The Netherlands) (excitation wavelength 365 nm, emission wavelength 590 nm) as described elsewhere (Karsten & Wollenberger, 1977). Bovine thymus DNA (Calbiochem) was used as a standard.

Statistical analysis

Data in the control and RV overload groups were analyzed using an unpaired Student *t*-test, corrected for multiple testing by Bonferroni's post hoc test. The distributions of myocyte area in both groups were tested for significant differences using the non-parametric MANOVA test (SPSS version 10, SPSS Inc., Chicago, IL, USA). PCNA-positive distributions in both groups were tested with a Chi-squared test. Data are expressed as mean $\pm$ SD. A P-value < 0.05 was considered statistically significant.

Results

General and cardiac characteristics of both groups studied are illustrated in Table 1. Due to increased RV pressures in lambs with RV overload, being as high as LV pressures, the ratio of RV to LV wall thickness was double that in control lambs. This was due to an increase in RV free wall thickness by 109% in the RV overload group, whereas LV wall thickness remained unchanged.

(Histo)morphometry

Tissue morphometry

The relative volume fractions of myocytes, myocyte nuclei, collagen and tissue gaps are summarized in Table 2. For the right ventricle, no significant differences between the

Table 1 Group characteristics

	Control	RV pressure overload	*P* (*)
n	5	5	–
Body weight (kg)	20.4 ± 3.0	16.6 ± 3.7	0.11
RV end-systolic pressure (mmHg)	12 ± 3	64 ± 8	**< 0.01**
LV end-systolic pressure (mmHg)	78 ± 15	66 ± 13	0.20
RV free wall thickness (mm)	4.5 ± 0.7	9.4 ± 0.6	**< 0.01**
LV free wall thickness (mm)	10.5 ± 0.7	10.2 ± 1.9	0.85
IVS thickness (mm)	14.0 ± 2.8	12.8 ± 0.84	0.37
RV/LV wall thickness ratio	0.43 ± 0.04	0.94 ± 0.15	**< 0.01**

Ventricular wall thicknesses were measured post-mortem.
RV, right ventricular; LV, left ventricular.
Data are expressed as mean ± SD.
*Unpaired Student's *t*-test: RV pressure overload vs. control. Bold type indicates a significant difference.

Table 2 Histomorphometric analysis of right and left ventricular myocardium of hearts from lambs with right ventricular overload and from control lambs

	RV			LV		
	Control	RV overload	*P* (*)	Control	RV overload	*P* (*)
Endocardial volumes (%)						
Myocytes	77.3 ± 6.1	72.2 ± 7.1	0.26	81.3 ± 6.8	77.9 ± 9.4	0.54
Myocyte nuclei	2.0 ± 0.4	2.1 ± 0.5	0.77	1.6 ± 0.3	2.3 ± 0.7	0.06
Collagen	6.4 ± 1.4	7.8 ± 5.5	0.87	4.2 ± 1.8	6.4 ± 1.5	0.57
Tissue gap	13.9 ± 3.2	14.6 ± 8.7	0.60	8.2 ± 4.6	10.3 ± 6.8	0.07
Rest	2.4 ± 4.1	5.4 ± 3.6	0.25	6.4 ± 3.3	5.4 ± 2.9	0.63
Mid-myocardial volumes (%)						
Myocytes	81.0 ± 3.2	78.4 ± 7.9	0.51	86.0 ± 3.9	83.5 ± 10.9	0.64
Myocyte nuclei	2.1 ± 0.9	2.0 ± 0.3	0.80	1.7 ± 0.2	2.4 ± 0.4	**< 0.05**
Collagen	7.4 ± 1.5	8.2 ± 5.3	0.75	4.5 ± 1.8	5.3 ± 2.3	0.46
Tissue gap	7.4 ± 4.2	8.1 ± 2.0	0.75	5.7 ± 2.5	8.2 ± 6.6	0.59
Rest	4.2 ± 4.0	5.3 ± 6.1	0.74	3.7 ± 2.1	3.0 ± 4.1	0.74
Epicardial volumes (%)						
Myocytes	73.3 ± 8.6	68.8 ± 10.8	0.48	82.3 ± 5.9	75.9 ± 8.7	0.21
Myocyte nuclei	1.9 ± 0.3	1.7 ± 0.2	0.20	1.7 ± 0.3	2.3 ± 0.6	**0.05**
Collagen	12.3 ± 2.8	14.5 ± 5.7	0.70	6.7 ± 2.4	8.3 ± 4.9	0.38
Tissue gap	9.9 ± 5.1	11.3 ± 5.7	0.45	6.5 ± 2.1	8.5 ± 4.3	0.53
Rest	4.5 ± 4.4	5.5 ± 4.7	0.74	4.6 ± 3.4	7.4 ± 3.3	0.23

The relative volume fractions of myocytes, myocyte nuclei, amount of collagen and tissue gaps in the LV and RV of the control group (left column) and RV pressure overload group (right column) are given. 'Rest' represents all structures other than those mentioned above (e.g. vasculature and fibroblasts). A distinction between epicardial, mid-myocardial and endocardial layers was based on different myocyte fiber orientation.
*Unpaired Student's *t*-test: RV overload vs. control. Bold type indicates a significant difference.

Table 3 Proportion of right ventricular (RV) myocyte binucleation and myocyte dimensions measured in individual myocytes which were obtained from hearts of lambs subjected to chronic RV overload and from hearts of control lambs

	% Binucleation	Length	Width	Area
Control hearts ($n = 5$)	59 ± 9	67.5 ± 9.1	11.6 ± 1.1	787 ± 162
RV overload hearts ($n = 5$)	47 ± 13	69.0 ± 8.1	12.1 ± 0.4	851 ± 117
*P**	0.12	0.78	0.38	0.49

RV myocyte dimensions (length, width) are given in μm. RV myocyte area is estimated by multiplying RV myocyte length and width and is given in μm^2.
*Unpaired Student's *t*-test: RV overload vs. control.

control group and the RV overload group were observed between all structures counted, including fibroblasts and vascular endothelium. These findings indicate that on a quantitative basis hardly any difference in percent composition of myocardial tissue exists between groups with and without chronic RV pressure overload. Thus chronic RV pressure overload appears to result in 'more of the same' myocardial tissue.

In the LV, a similar pattern was seen except for significant differences of the relative volume fraction of myocyte nuclei in the mid-myocardial and epicardial layers, being higher in hearts with RV overload than in control hearts.

Cellular morphometry

The results of morphometric analysis of individual RV myocytes in both groups are summarized in Table 3. No significant differences in average RV myocyte length, width or area between both groups were found indicating unchanged average myocyte shape. The distribution of myocyte size in both populations is comparable, as indicated by the almost overlapping myocyte area distributions in Fig. 1.

Normal sheep RV myocardium is composed of both mononucleated as well as binucleated myocytes. A typical example of both myocyte types is presented in Fig. 2. After chronic RV pressure overload, the relative numbers of

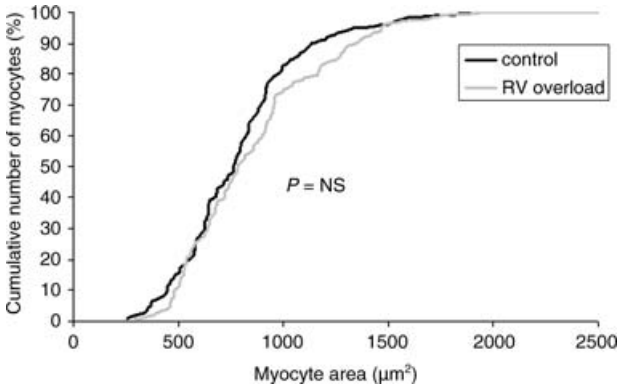

Fig. 1 Cumulative percentage of RV myocytes as a function of myocyte size. The black line represents the control group whereas the grey line represents the RV overload group. Chronic RV pressure overload does not result in a shift of the curve, which indicates that myocyte size is not affected by increased afterload.

mono- and binucleated myocytes did not differ significantly from those of the control group (Table 3).

Immunohistochemistry

Cardiac myocyte proliferation

A total of 21 slides were made, including a positive control (human tonsil) and a negative control (normal RV sheep myocardium without primary antibody). Figure 3 shows a typical example of a slide from each group after PCNA staining. From these slides, 252 photographs were taken randomly, 138 from the control group and 114 from the RV overload group. PCNA-positive myocyte nuclei were observed in both the control group (14.5% of photographs analyzed) and in the RV overload group (21.9% of photographs analyzed) although the frequency of PCNA-positive myocyte nuclei per photograph was rather low in all myocardial samples analyzed (maximal values up to 0.016 and 0.033 in the control group and RV overload group, respectively). Figure 4 shows the distribution of the fraction of PCNA-positive myocyte nuclei per photograph in both groups. A significant rightward shift of the distribution curve occurs after chronic RV pressure overload, indicating a higher degree of myocyte proliferation in this group ($P = 0.01$).

Cardiac DNA concentration

Table 4 illustrates the average myocardial DNA concentration in each tissue sample (μg DNA mg^{-1} tissue). No significant differences were found between the two groups with regard to myocardial DNA concentration in the RV free wall, LV free wall or IVS.

Discussion

The results of this study show that RV free wall thickness is increased by 109% after chronic RV pressure overload, applied to neonatal sheep hearts. No significant changes were found for myocardial tissue composition expressed

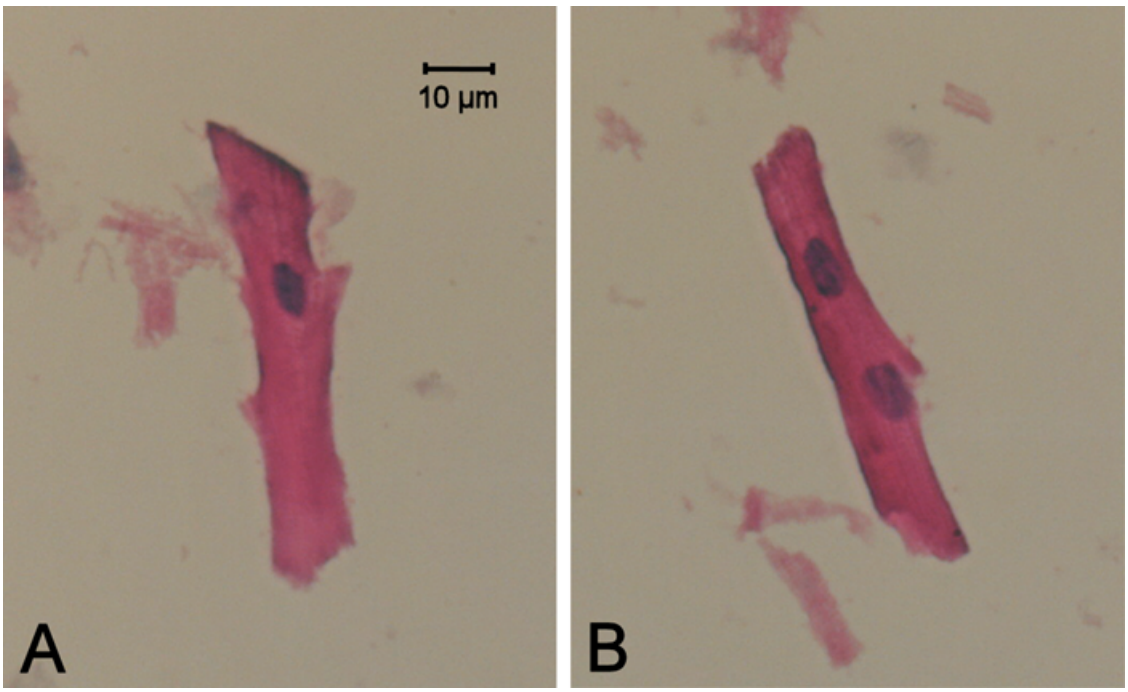

Fig. 2 Typical examples of isolated right ventricular mononucleated (A) and binucleated (B) myocytes, representative for both groups. Myocyte dimensions and proportion of binucleation were not significantly different between the two groups (Table 3).

Table 4 Myocardial DNA concentrations determined in right ventricular (RV), left ventricular (LV) and interventricular septum (IVS) myocardium from hearts of lambs with right ventricular overload and from hearts of control lambs

	RV samples (μg DNA mg^{-1} tissue)	LV samples (μg DNA mg^{-1} tissue)	IVS samples (μg DNA mg^{-1} tissue)
Control hearts ($n = 5$)	3.72 ± 0.62	3.76 ± 0.55	3.13 ± 0.22
RV overload hearts ($n = 4$)	3.44 ± 0.51	3.27 ± 0.23	3.36 ± 0.39
P*	0.50	0.14	0.31

*Unpaired Student's *t*-test: RV overload vs. control.

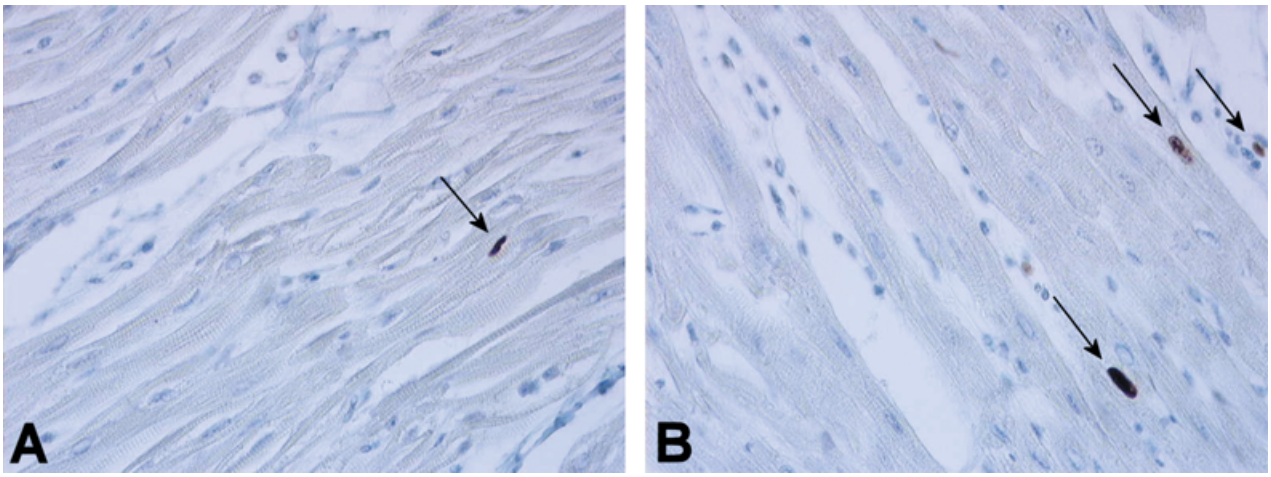

Fig. 3 Examples of right ventricular myocardium from control (A) and RV pressure overloaded (B) hearts stained for the presence of PCNA-positive nuclei. Image dimensions are 0.25 × 0.19 mm (width, height). Arrows indicate PCNA-positive nuclei.

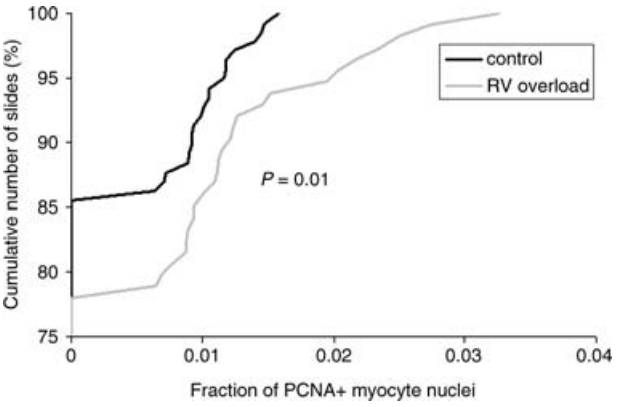

Fig. 4 Relative cumulative percentage of the fraction of PCNA-positive myocytes determined in 138 photographs of right ventricular myocardium in the control group (black line) and in 114 photographs of right ventricular myocardium in the RV overload group (grey line). Note that chronic RV pressure overload resulted in a significant rightward shift of the curve, indicating an increase in PCNA expression in this group.

as volume percentages, individual myocyte dimensions, the degree of myocyte nucleation or myocardial DNA content between groups with and without chronic RV pressure overload. A significant increase, however, was found for the number of PCNA-positive myocyte nuclei in the RV overload group ($P = 0.01$).

RV wall thickness may theoretically be increased by two mechanisms. Either new myocytes are added (hyperplastic growth) or existing cells are increased in size without the formation of new myocytes (hypertrophic growth). In addition, experimental studies have shown that both mechanisms may coexist. For example, Sedmera & colleagues (2003) have shown that left ventricular pressure loading by aortic constriction in rats may trigger both a hyperplastic and a hypertrophic response later on. However, myocardial analysis, if both mechanisms are present at the same time, is difficult in terms of methodology, as will be discussed below.

For many years the dogma was that hyperplastic growth occurred during fetal development only. Shortly after birth, when cardiac myocytes are terminally differentiated, a complete transition from a hyperplastic to a hypertrophic growth pattern is thought to occur (Rakusan, 1984). Recently, the concept of the heart being a terminally differentiated organ as it excludes any turnover of myocytes has been questioned (Nadal-Ginard et al. 2003). Under certain circumstances in the adult heart, myocytes are able to re-activate their cell cycle, which initiates a secondary hyperplastic growth response (Clubb et al.

1986; Poolman et al. 1999; Pasumarthi & Field, 2002). For instance, increased hemodynamic load due to exposure to carbon monoxide in fetal rats has been shown to result in cardiomegaly because of increased myocyte hyperplasia. This hyperplastic response is sustained throughout the early neonatal period (Clubb et al. 1986). In mice lacking a specific cyclin-dependent kinase inhibitor ($p27^{kip1}$), prolonged proliferation of cardiac myocytes and perturbation of myocyte hypertrophy was found (Poolman et al. 1999).

Several authors have emphasized that the evaluation of the adaptive myocardial responses to increased loading conditions is severely hampered by methodological difficulties (Olivetti et al. 1994; Nadal-Ginard et al. 2003). Many of the parameters used are not exclusively representative for either hypertrophy or hyperplasia. For example, proliferating cellular nuclear antigen (PCNA) is a 36-kD nuclear protein which is expressed specifically in cell nuclei during the S-phase of the cell cycle, immediately before DNA synthesis (Marino et al. 1991). As such it is considered to be a marker of cellular proliferation (Matturri et al. 2002; Nadal-Ginard et al. 2003). The downside of using this protein as a marker, however, is that it merely indicates DNA synthesis, irrespective of whether the synthesis is followed by cellular division (as occurs in hyperplasia) or not. Therefore, expression of PCNA by itself cannot be used to distinguish between myocardial hypertrophy and myocardial hyperplasia. Furthermore, in the event of a hypertrophic response, enlargement of existing myocytes would result in an increased volume fraction of myocytes and, via simple 'dilution', in a decreased volume fraction of myocyte nuclei and in a decreased DNA content per gram of tissue (van der Laarse et al. 1989). However, this can only be true if the number of nuclei per myocyte and the degree of nuclear ploidy remain constant (van der Laarse et al. 1989). Several studies have shown that in case of hypertrophic myocardial growth, an increase in nuclear size is observed which is found to be directly related to the formation of polyploid nuclei and an increase in DNA content (Vliegen et al. 1990; Capasso et al. 1992). Making a judgment based on isolated calculations of the number of myocyte nuclei may yield false conclusions: a constant density of myocyte nuclei may indicate a hyperplastic response ('more of the same tissue') but it may also be the result of a combination of 'dilution' due to myocyte enlargement (hypertrophy) in combination with the occurrence of karyokinesis without cytokinesis (binucleation), as has been shown to occur in a hypertrophic response (Anversa & Kajstura, 1998; Clubb & Bishop, 1984). Therefore it has been stated that, so far, the quantitative determination of myocyte nuclei, combined with the evaluation of the distribution of nuclei in myocytes, appears to be the only approach available for the documentation of myocyte cellular hyperplasia in the myocardium (Anversa et al. 1990).

When we refer to our own measurements, the rightward shift of the curve in Fig. 4 signifies myocyte DNA synthesis in the pressure overloaded RV myocardium. In combination with our other results of unchanged DNA concentration (expressed per mg of myocardial tissue), unchanged degree of binucleation, and unchanged tissue composition (no substantial myocardial scar formation as has previously been shown to occur in pressure overload hypertrophy; Doering et al. 1988; Thiedemann et al. 1983; Vliegen et al. 1991), we can conclude that the DNA synthesis is the result of a hyperplastic instead of a hypertrophic reaction.

With regard to the left ventricle, significant increases in myocyte nuclear density were also found in two of the three layers of left ventricular myocardium (see Table 2). Although this was an unexpected finding, similar findings have been reported in the literature. Sedmera and colleagues studied the responses of neonatal rat left ventricle to pressure overload, induced by aortic constriction (Sedmera et al. 2003). Apart from significant increases in LV mass and myocyte width, a mild but significant increase was found in RV wall mass and RV myocyte width in the group characterized by severe cardiomegaly 21 days after aortic constriction. With regard to the present study, it might be hypothesized that the increased RV pressure, by means of direct ventricular interaction via the interventricular septum, triggers a nuclear proliferative response in LV myocytes. In addition, non-uniformity of myocyte proliferation throughout the ventricular wall has been reported to occur in both mammals as well as in birds: from outside to inside a decreasing gradient of DNA synthesis has been reported to occur in the ventricular wall (Jeter et al. 1971; Sedmera et al. 2002). This finding might provide an explanation as to why the epicardial and mid-myocardial layers of the left ventricle show a significant increase in myocyte nuclear proliferation only.

One of the few papers that has studied the effects of RV pressure overload on sheep myocardium is the study by Barbera et al. (2000). They created a model in which fetal hearts were subjected to an increase in RV pressure for a period of 10 days, obtained by pulmonary artery constriction. Based on cytomorphometric data they calculated that RV pressure overload had resulted in a 50% increase in myocyte number in RV myocardium. In addition, a significant increase in RV myocyte length was found, whereas myocyte width remained constant. Myocyte volume, expressed as a percent of total tissue volume, significantly increased from $75.5 \pm 1.3\%$ in the control group to $81.8 \pm 4.6\%$ in the RV overload group ($P < 0.05$). Based on volumetric calculations using a cylindrical model, they found a 36% increase in myocyte volume. This finding led them to conclude that besides a hyperplastic response, the fetal myocytes showed a hypertrophic response as well.

When analyzing our own data, no significant increases in tissue composition or individual myocyte dimensions were found. This discrepancy with regard to the results of Barbera et al. (2000) may be related to the fact that the timing of pressure overload differs between that

study and ours. Estimations of myocyte volumes in our study, based on the cylindrical model as described above (Barbera et al. 2000), results in average myocyte volumes of 71 300 μm^3 in the control group and 79 300 μm^3 in the pressure overload group. Taken together, as compared to the control group, chronic RV pressure overload resulted in an increase in myocyte volume by approximately 11%. As this increase in volume is not unexpected in a neonatal phase of the heart, this (hypertrophic) cellular enlargement does not account for the enormous increase in wall thickness (i.e. 109%). Furthermore, if it is hypothesized that a pure hypertrophic response had occurred, the volume% of myocytes (see Table 2) should have increased and the volume% of myocyte nuclei should have decreased (dilution) as the degree of binucleation did not significantly differ between both groups (Table 3). Therefore, although a contributing effect of myocardial hypertrophy cannot be excluded completely, the vast majority of the increase in RV wall thickness is due to a hyperplastic response.

The last known confounding factor in the analysis of myocardial responses to ventricular overload is the occurrence of myocardial cell death (Kajstura et al. 1995; Narula et al. 1996; Olivetti et al. 1997). This may occur via either myocyte necrosis or apoptosis. The former reaction is associated with an inflammatory reaction, fibroblast activation, vessel proliferation and, ultimately, scar formation (Nadal-Ginard et al. 2003). This type of cell death is not likely to have occurred in our study as this would have led to different morphometric results (see Table 2). Myocyte apoptosis, on the other hand, does not result in tissue fibrosis; dying myocytes are removed by neighboring cells in the absence of an inflammatory reaction (MacLellan & Schneider, 1997). Apoptotic cells may either be replaced by new myocytes or neighboring myocytes may take their place by means of hypertrophy. In the latter case, this would have resulted in a group of larger myocytes and thus in a rightward shift of the curve presented in Fig. 1. In the case of replacement, the occurrence of apoptosis would even have underestimated the degree of myocyte hyperplasia.

Another possibility for the occurrence of RV myocyte hyperplasia after chronic RV pressure overload that should be considered is suggested by the study of Kajstura & colleagues (1995). They have shown that cardiac apoptosis occurs postnatally only and that the frequency of apoptosis is higher in the RV than in the LV and interventricular septum (Kajstura et al. 1995). This finding is ascribed to RV unloading that occurs shortly after birth due to expansion of the pulmonary vascular bed. In their study, it has been suggested that this pressure unloading may enhance apoptosis in the RV. This mechanism would explain the normal difference between RV and LV wall thickness. Conversely, it may be hypothesized that in the setting of increased RV afterload, the frequency of apoptosis is decreased. Although it is unlikely that an increase in RV wall thickness of 109% is solely due to a decrease in apoptosis in the setting of increased RV afterload, a contribution to the observed hyperplastic response in our study cannot be excluded on the basis of our results.

After 8 weeks of chronic RV pressure overload and independently of the increase in RV wall thickness, right ventricular contractile function has been found to be significantly increased (Leeuwenburgh et al. 2001). Despite this increase, global pump function was found to be decreased, which has been related to an increase in RV diastolic stiffness (Leeuwenburgh et al. 2002). The hyperplastic myocardial response as presented in the current study may be hypothesized to provide, through the process of ventricular thickening, an explanation for this increase in diastolic stiffness.

Conclusions

The results of our study indicate that chronic RV pressure overload applied at a young age in sheep is accompanied by a considerable increase in RV wall thickness. Both the morphometric composition of overloaded RV myocardium as well as the myocardial DNA concentration are unchanged. In addition, the proportion of myocyte multi-nucleation is not significantly different from that of normal myocardium, although significantly more myocyte nuclei were found to be PCNA-positive. These findings indicate that the neonatal lamb heart primarily responds to increased workload by means of myocyte hyperplasia. In newborn patients with congenital heart disease, this type of adaptive response might affect ventricular function by means of myocardial remodelling.

References

Anversa P, Kajstura J (1998) Ventricular myocytes are not terminally differentiated in the adult mammalian heart. *Circ Res* **83**, 1–14.

Anversa P, Palackal T, Sonnenblick EH, Olivetti G, Meggs LG, Capasso JM (1990) Myocyte cell loss and myocyte cellular hyperplasia in the hypertrophied aging rat heart. *Circ Res* **67**, 871–85.

Anversa P, Capasso JM, Olivetti G, Sonnenblick EH (1992) Cellular basis of ventricular remodeling in hypertensive cardiomyopathy. *Am J Hypertens* **5**, 758–70.

Astorri E, Chizzola A, Visioli O, Anversa P, Olivetti G, Vitali-Mazza L (1971) Right ventricular hypertrophy – a cytometric study on 55 human hearts. *J Mol Cell Cardiol* **2**, 99–110.

Barbera A, Giraud GD, Reller MD, Maylie J, Morton MJ, Thornburg KL (2000) Right ventricular systolic pressure load alters myocyte maturation in fetal sheep. *Am J Physiol Regul Integr Comp Physiol* **279**, R1157–64.

Becker AE (1993) Myocardial hypertrophy and hyperplasia. A narrative of past, present and future. *Eur Heart J* **14**, 1–3.

Beinlich CJ, Rissinger CJ, Morgan HE (1995) Mechanisms of rapid growth in the neonatal pig heart. *J Mol Cell Cardiol* **27**, 273–81.

Bishop SP, Hine P (1975) Cardiac muscle cytoplasmic and nuclear development during canine neonatal growth. In *Recent Advances in Studies on Cardiac Structure and Metabolism* (ed. Roy P), **vol. 8**, pp. 77–98. Baltimore: University Press.

Capasso JM, Bruno S, Cheng W, Li P, Rodgers R, Darzynkiewicz Z, Anversa P (1992) Ventricular loading is coupled with DNA synthesis in adult cardiac myocytes after acute and chronic myocardial infarction in rats. *Circ Res* **71**, 1379–89.

Clubb FJ Jr, Bishop SP (1984) Formation of binucleated myocardial cells in the neonatal rat. An index for growth hypertrophy. *Lab Invest* **50**, 571–7.

Clubb FJ Jr, Penney DG, Baylerian MS, Bishop SP (1986) Cardiomegaly due to myocyte hyperplasia in perinatal rats exposed to 200 ppm carbon monoxide. *J Mol Cell Cardiol* **18**, 477–86.

Doering CW, Jalil JE, Janicki JS, Pick R, Aghili S, Abrahams C, et al. (1988) Collagen network remodelling and diastolic stiffness of the rat left ventricle with pressure overload hypertrophy. *Cardiovasc Res* **22**, 686–695.

Gerdes AM (2002) Cardiac myocyte remodeling in hypertrophy and progression to failure. *J Card Fail* **8**, S264–8.

Grajek S, Lesiak M, Pyda M, Zajac M, Paradowski S, Kaczmarek E (1993) Hypertrophy or hyperplasia in cardiac muscle. Postmortem human morphometric study. *Eur Heart J* **14**, 40–47.

Jeter JR Jr, Cameron IL (1971) Cell proliferation patterns during cytodifferentiation in embryonic chick tissues: liver, heart and erythrocytes. *J Embryol Exp Morphol* **25**, 405–22.

Kajstura J, Mansukhani M, Cheng W, Reiss K, Krajewski S, Reed JC, et al. (1995) Programmed cell death and expression of the protooncogene bcl-2 in myocytes during postnatal maturation of the heart. *Exp Cell Res* **219**, 110–121.

Karsten U, Wollenberger A (1977) Improvements in the ethidium bromide method for direct fluorometric estimation of DNA and RNA in cell and tissue homogenates. *Anal Biochem* **77**, 464–470.

van der Laarse A, Hollaar L, Vliegen HW, Egas JM, Dÿkshoom NJ, Cornelisse CJ, et al. (1989) Myocardial (iso)enzyme activities, DNA concentration and nuclear polyploidy in hearts of patients operated upon for congenital heart disease, and in normal and hypertrophic adult human hearts at autopsy. *Eur J Clin Invest* **19**, 192–200.

Leeuwenburgh BPJ, Helbing WA, Steendijk P, Schoof PH, Baan J (2001) Biventricular systolic function in young lambs subject to chronic systemic right ventricular pressure overload. *Am J Physiol Heart Circ Physiol* **281**, H2697–H2704.

Leeuwenburgh BPJ, Steendijk P, Helbing WA, Baan J (2002) Indexes of diastolic RV function: load dependence and changes after chronic RV pressure overload in lambs. *Am J Physiol Heart Circ Physiol* **282**, H1350–H1358.

Li F, Wang X, Capasso JM, Gerdes AM (1996) Rapid transition of cardiac myocytes from hyperplasia to hypertrophy during postnatal development. *J Mol Cell Cardiol* **28**, 1737–46.

MacLellan WR, Schneider MD (1997) Death by design. Programmed cell death in cardiovascular biology and disease. *Circ Res* **81**, 137–44.

Marino TA, Haldar S, Williamson EC, Beaverson K, Walter RA, Marino DR, et al. (1991) Proliferating cell nuclear antigen in developing and adult rat cardiac muscle cells. *Circ Res* **69**, 1353–60.

Matturri L, Milei J, Grana DR, Lavezzi AM (2002) Characterization of myocardial hypertrophy by DNA content, PCNA expression and apoptotic index. *Int J Cardiol* **82**, 33–9.

Nadal-Ginard B, Kajstura J, Leri A, Anversa P (2003) Myocyte death, growth, and regeneration in cardiac hypertrophy and failure. *Circ Res* **92**, 139–50.

Narula J, Haider N, Virmani R, DiSalvo TG, Kolodgie FD, Hajjar RJ, et al. (1996) Apoptosis in myocytes in end-stage heart failure. *N Engl J Med* **335**, 1182–9.

Norton AJ (1993) Microwave oven heating for antigen unmasking in routinely processed tissue sections. *J Pathol* **171**, 79–80.

Olivetti G, Ricci R, Anversa P (1987) Hyperplasia of myocyte nuclei in long-term cardiac hypertrophy in rats. *J Clin Invest* **80**, 1818–21.

Olivetti G, Ricci R, Lagrasta C, Maniga E, Sonnenblick EH, Anversa P (1988) Cellular basis of wall remodeling in long-term pressure overload-induced right ventricular hypertrophy in rats. *Circ Res* **63**, 648–657.

Olivetti G, Melissari M, Balbi T, Quaini F, Sonnenblick EH, Anversa P (1994) Myocyte nuclear and possible cellular hyperplasia contribute to ventricular remodeling in the hypertrophic senescent heart in humans. *J Am Coll Cardiol* **24**, 140–9.

Olivetti G, Abbi R, Quaini F, Kajstura J, Cheng W, Nitahara JA, et al. (1997) Apoptosis in the failing human heart. *N Engl J Med* **336**, 1131–41.

Oparil S, Bishop SP, Clubb FJ Jr (1984) Myocardial cell hypertrophy or hyperplasia. *Hypertension* **6**, III38–43.

Pasumarthi KB, Field LJ (2002) Cardiomyocyte cell cycle regulation. *Circ Res* **90**, 1044–54.

Poolman RA, Li JM, Durand B, Brooks G (1999) Altered expression of cell cycle proteins and prolonged duration of cardiac myocyte hyperplasia in p27KIP1 knockout mice. *Circ Res* **85**, 117–27.

Rakusan K (1984) Cardiac growth, maturation and aging. In *Growth of the Heart in Health and Disease* (ed. Zak R), pp. 131–164. New York: Raven.

Saiki Y, Konig A, Waddell J, Rebeyka IM (1997) Hemodynamic alteration by fetal surgery accelerates myocyte proliferation in fetal guinea pig hearts. *Surgery* **122**, 412–9.

Sedmera D, Hu N, Weiss KM, Keller BB, Denslow S, Thompson RP (2002) Cellular changes in experimental left heart hypoplasia. *Anat Rec* **267**, 137–45.

Sedmera D, Thompson RP, Kolar F (2003) Effect of increased pressure loading on heart growth in neonatal rats. *J Mol Cell Cardiol* **35**, 301–9.

Thiedemann KU, Holubarsch C, Medugorac I, Jacob R (1983) Connective tissue content and myocardial stiffness in pressure overload hypertrophy. A combined study of morphologic, morphometric, biochemical, and mechanical parameters. *Basic Res Cardiol* **78**, 140–155.

Vliegen HW, Bruschke AV, Van der Laarse A (1990) Different response of cellular DNA content to cardiac hypertrophy in human and rat heart myocytes. *Comp Biochem Physiol A* **95**, 109–14.

Vliegen HW, van der Laarse A, Cornelisse CJ, Eulderink F (1991) Myocardial changes in pressure overload-induced left ventricular hypertrophy. A study on tissue composition, polyploidization and multinucleation. *Eur Heart J* **12**, 488–494.

Weibel ER (1979) In *Stereological Methods, vol. 1: Practical Methods for Biological Morphometry*. London: Academic Press.